

STRUCTURAL DESIGN OF HYBRID STRUCTURE WITH CLT SEISMIC PANELS AND STEEL FRAME

Kouji Fukumoto¹, Marina Koda², Hiroshi Isoda³

ABSTRACT: We have developed a new hybrid structural system with fire-resistance performance, combining CLT infill panels and a steel frame, for middle- and high-rise buildings. This structural system draws out the potential structural performance of CLT panels by holding them in the steel frames. Steel frames, without considering CLT panels, can support gravity loads of a high-rise building during fires so that it may be possible to omit the fireproof covering of the CLT panels and to specialize CLT panels to support seismic forces. This paper shows the details of the developed hybrid system as well as the seismic design and fire resistance experimental result, with an actual example project.

KEYWORDS: CLT, Steel frame, Hybrid structure, Seismic panel, Seismic performance, Fire-resistance performance

1 INTRODUCTION

Since the Japanese government notification related to CLT (Cross Laminated Timber) was enforced in 2016, the manuals on design have been developed [1], and the buildings using CLT are becoming more and more in use in Japan as well as in other countries. The high-rise buildings utilizing CLT (for example, Reference [2]) have been already constructed in Europe and North America where CLT is in widespread use prior to other countries. In Japan as well, the efforts to apply timber structures to middle- and high-rise buildings have become active. Although CLT is expected to be usable as leading structural material for that purpose, currently, its use for middle- and large-scale buildings has not been widespread partly because of the needs to meet higher seismic standards and fire protection standards than in other countries.

Under the circumstances, the authors had an opportunity, in 2018, to design the structure of the Hyogo Forestry Hall, a five-story office building aimed at becoming a model for encouraging broad use of CLT by making effective use of CLT.

However, in case of using a CLT panel construction method in an urban central area like Kobe City, fireproof covering for timber structural members to meet the requirement for ensuring the one-to-three-hour fire resistance performance according to the application area and scale of the building as specified in the Building Standards Act of Japan not only conflicts with the architectural request for representing wood in a space but also raises issues of labour and cost for installing fireproof covering. Thus, securing the fire-resistance performance of a timber structure involves multifaceted issues.

Furthermore, large-section glued laminated timber is required to achieve a large span exceeding 10 meters necessary for a work space of office with a timber structure. If fire resistive glued laminated timber is used for that purpose, it would be more disadvantageous in terms of cost.

Besides, application of CLT to high-rise buildings is difficult because if CLT is used as seismic structural elements in a timber frame as has been before or if a structure is assembled only with CLT panels, the surrounding timber frame will fail before CLT exhibits its strength to the full as shown in Figure 1. Moreover, with the CLT panel construction method or a structural system in combination with the conventional timber structure, it will be difficult to rationally attain high axial force retention and a large span frame which are indispensable to a high-rise building, with consideration for economical efficiency as well.

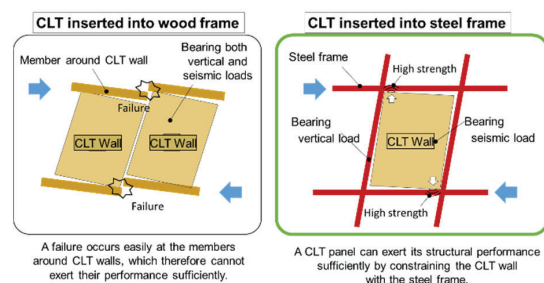


Figure 1: CLT panels inserted into steel frame

Therefore, the authors had an eye on a structural system with CLT as seismic structural elements built in a steel

¹ Kouji Fukumoto, Associate Professor, Okayama University, Japan, k.fukumoto@okayama-u.ac.jp (Former position: Structural Engineering Section, TAKENAKA Corporation, Japan)

² Marina Koda, Structural Engineering Section, TAKENAKA Corporation, Japan, marina.kouda@takenaka.co.jp

³ Hiroshi Isoda, Professor, Research Institute for Sustainable Humansphere, Kyoto University, Japan, hisoda@rish.kyoto-u.ac.jp

structure as reported in [3], which was aimed at achieving high axial force retention and a large span rationally and economically through a steel structural frame by constraining CLT with the steel frame and thereby letting CLT exhibiting its inherent structural performance. Additionally, we specialized CLT panels as seismic structural elements and eliminated the need for fireproof covering to improve the design, workability and economic efficiency.

This paper presents the structural design method taking an actual project, and also shows the verification results of the effect of the combustion of CLT on the fire-resistance performance of the surrounding steel in case without fireproof covering for CLT seismic panels in order to ensure the fire-resistance performance of the structural system. Furthermore, the paper reports the construction condition focused on the joints.

2 STRUCTURAL DESIGN METHOD IN “HYOGO FORESTRY HALL”

2.1 OUTLINE OF STRUCTURAL SYSTEM

Figure 2 shows the outline of the Hyogo Forestry Hall, a case of the authors' design, and Figure 3 shows a structure rendering of the same building. As shown in Figure 4, the

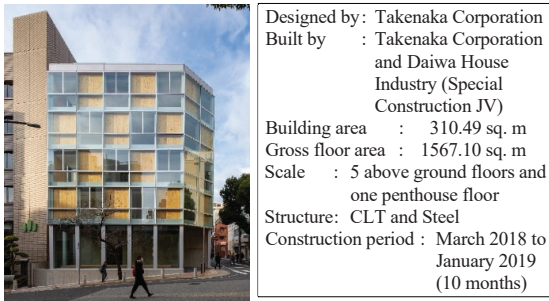


Figure 2: Outline of Hyogo Forestry Hall

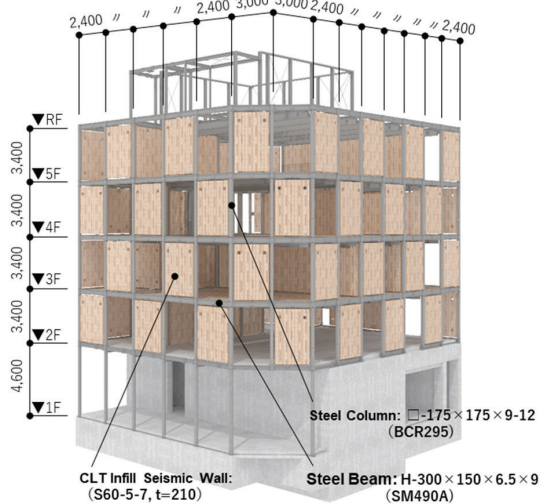


Figure 3: Structure rendering

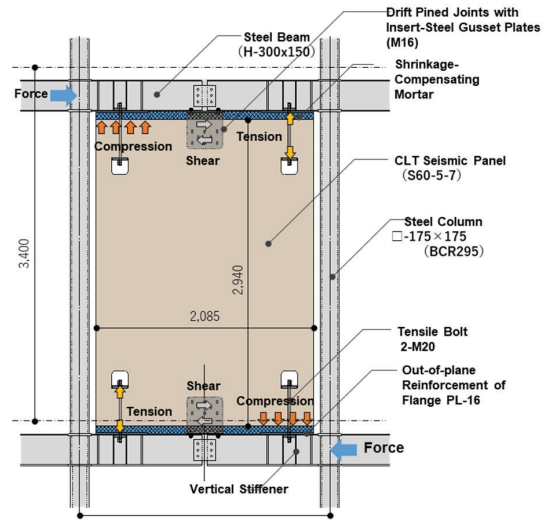


Figure 4: CLT panel inserted in steel frame

standard configuration consists of a CLT infill seismic wall S60-5-7 (210 mm thick with 5 layers and 7 plies), steel columns (□-175x175x9, BCR295) and steel beams (H-300x150x6.5x9, SM490A). A CLT seismic panel, 2.940 m high and 2.085 m wide (H/L=1.41), is placed on a steel grid at the floor height of 3.4 m with columns arranged at a spacing of 2.4 m. Tensile bolts 2-M20 (ABR400) are placed at four corners of a CLT panel for the tensile joints, while the drift pinned joints with insert-steel gusset plates (drift pin diameter 16 mm) are provided at the center for the shear joints. We also filled the space between CLT panels and steel beams with shrinkage-compensating mortar to make sure of the later described fire-resistance performance and stress transmission.

2.2 RELATIONS BETWEEN JOINT STRENGTH AND SHEAR FORCE BORNE BY CLT INFILL SEISMIC WALL

Table 1 shows the relations between the joint strength and the shear force borne by CLT panels in the above structural system. The horizontal strength depends upon the equilibrium between the moment by the couple of vertical forces due to the yield tension strength of tensile bolts (T_y) and the bearing strength of the upper and lower bearing area (C_u) and the moment by the couple of shear forces (Q_u) in upper and lower shear joints caused by horizontal forces as shown in Figure 5. The CLT panel was S60-5-7 (210 mm thick), however the compressive strength of the bearing area was assumed to be S60-5-5 (150 mm thick) by not considering the outermost plies since the beam flange was 150 mm wide.

The analytical result indicated that the transmission of the compression stress in the bearing area of CLT panels that depends upon the shear yield strength of boundary beams (Q_v) was 56% of that in case of depending upon the bearing strength of CLT panels (C_c). In that case, assuming that the tensile bolts have tensile-yielded simultaneously, the shear stress of CLT panels (τ) is 0.62 N/mm². However, the tensile yield strength was set for tensile bolts to prevent prior failure at the position around

a square hole in a CLT panel as shown by the dotted line in Figure 6. Its contribution rate to the whole horizontal force ($M_{Ty}/\Sigma M_R$) is 23.3% when calculated using the rotational resistances in Table 1.

This project is also intended to minimize steel members by utilizing the structural performance of CLT panels. However, the section of steel beams can be increased to further increase the bearing force of CLT. Although the steel beam flanges receive the out-of-plane force due to the bearing force from CLT panels, vertical stiffeners are installed on the beams as shown in Figure 4. The compression stress from CLT panels is designed to allow the shear yield of steel beams. These vertical stiffeners also help prevent the steel beam web plates from shear buckling.

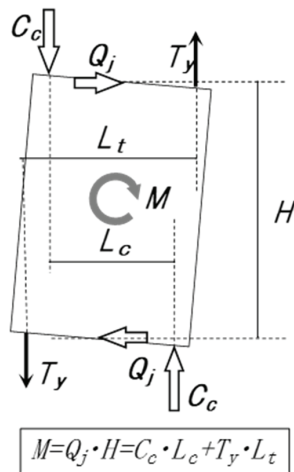


Figure 5: Conceptual diagram of rotational resistance

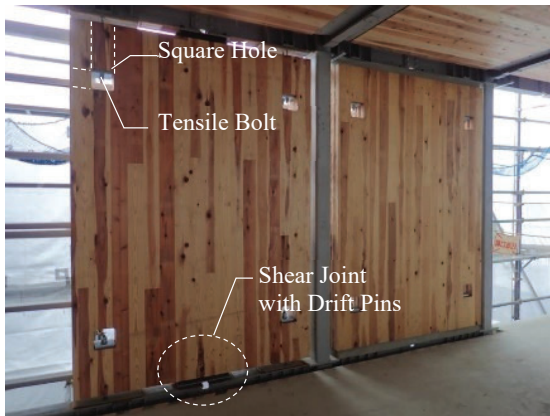


Figure 6: Joints of CLT panels

2.3 DESIGNING OF SHEAR JOINTS

The drift pinned joints with insert-steel gusset plates were applied for the shear joints. The hybrid structure with CLT seismic panels and a steel frame can account for the frictional force effectively because the structure system makes the compression stress predominant by constraining CLT panels.

Thus, this study considers the horizontal resistance force caused by frictional force with the coefficient of 0.3.

Table 1: Rotational resistances of CLT infill seismic walls in Hyogo Forestry Hall

CLT wall	Height	H	2940 (mm)
	Width	L	2085 (mm)
	Thickness	t	210 (mm)
	Strength Classification		S60-5-7
	In-plane bending strength	F_b	11.6 (N/mm ²)
CLT wall	In-plane shear strength	F_s	2.3 (N/mm ²)
	Apparent Strength Classification		S60-5-5
	Compressed area thickness	t_c	150 (mm)
Steel beam	In-plane compressive strength	F_c	9.72 (N/mm ²)
	Section		H-300x150x6.5x9
	Tensile yield point strength	F_t	357.5 (N/mm ²)
Steel beam	Shear yield strength	F_s	206.4 (N/mm ²)
	Shear sectional area	A_s	1833 (mm ²)
	Tensile bolt	Material	
Yield point strength		σ_y	235 (N/mm ²)
Diameter			M20
Quantity		n	2 (pcs.)
Tensile bolt	Sectional area	a_t	490 (mm ²)
	Tensile bolt position	d_t	230 (mm)
	$L - d_t$	d	1855 (mm)
	Bearing area width[1]	$0.25d$	463.8 (mm)
	Compression resultant force position	d_c	231.9 (mm)
	Bearing area effective sectional area	A_e	69563 (mm ²)
	Distance between couple of compression forces	L_c	1621 (mm)
	Distance between couple of tensile forces	L_t	1625 (mm)
	Bearing strength of CLT wall	C_c	676.1 (kN)
	Compressive strength of beam inclined to grain	C_{cv}	- (kN)
	Shear strength of beam	Q_v	378.3 (kN)
	Min. strength of CLT bearing area	C_u	378.3 (kN)
	Yield strength of tensile bolt	T_y	115.2 (kN)
	Rotational resistance due to C_{cu}	M_{Ccu}	613.4 (kN·m)
	Rotational resistance depending on T_y	M_{Ty}	187.1 (kN·m)
Full rotational resistance	ΣM_R	800.5 (kN·m)	
CLT horizontal strength	Q_R	272.3 (kN)	
CLT shear stress	τ_R	0.622 (N/mm ²)	
CLT shear reference strength	F_s	2.700 (N/mm ²)	

The structural performance of drift pins was designed by using the results of the previous joint experiment [4] using CLT panels (S60-5-5) and drift pins, 16 mm in diameter. In addition, considering the strength reduction coefficient 0.8 for arrangement of one row of several pins, the yield shear force per piece of drift pin, 16 mm in diameter, (q_{dpy}) was set to 22.7 kN per piece, and the initial stiffness (K_s) was set to 13.0 kN/mm per piece.

The design had an enough allowance for the primary design stage. The number of drift pins was determined so that the displacement of shear joint element springs under

the horizontal load-carrying capacity might not exceed the ultimate displacements at the shear joints as later described. The authors have reached the conclusion, through the above described designing process, that the shear stress (τ) that the CLT seismic panels can bear is 0.62 N/mm^2 .

2.4 FLOW OF STRUCTURAL DESIGN

Figure 7 shows the structural design flow of the Hyogo Forestry Hall. For this building, the allowable stress for sustained loading was designed without CLT seismic panels to specialize them as seismic structural elements. On that condition, we went through the following processes in a sequential order in compliance with the Seismic Calculation Route 3 as a steel structure under the Building Standards Act of Japan: Designing of the allowable stress for sustained and temporary loading; checking of the story deformation angles, modulus of eccentricity and story stiffness ratio; calculation of the horizontal load-carrying capacity; and checking of the ultimate displacements at the joints. Since the required horizontal load-carrying capacity has not been calculated in the previous studies, this study reduced the whole building to an equivalent single-degree-of-freedom system and then used a method of calculating the reduction rate of the required horizontal load-carrying capacity (structural characteristics factor: D_s) from the ductility factor on the assumption of the property of energy conservation.

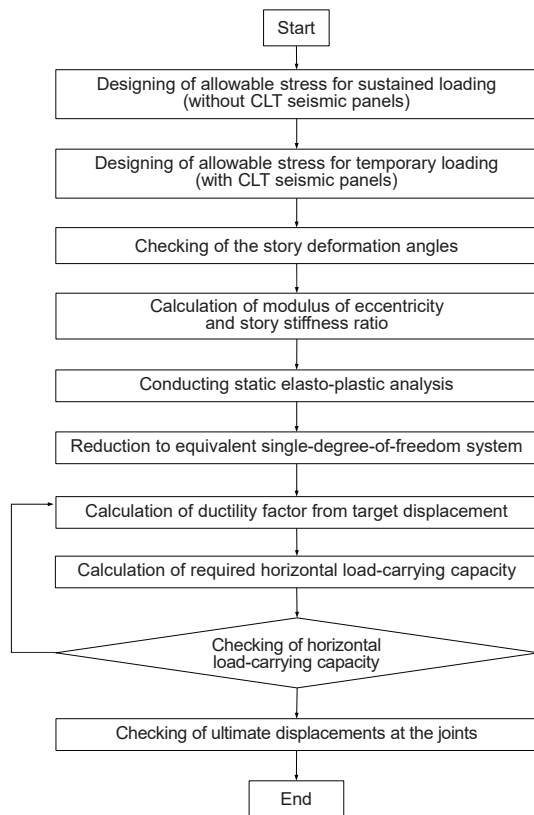


Figure 7: Flow of structural design

2.5 STRESS ANALYSIS MODEL

Figure 8 shows a stress analysis model of the Hyogo Forestry Hall. CLT panels were replaced by equivalent linear materials, which were analyzed as elastic bodies. The upper and lower ends of the wall had rigid beams as wide as the wall, and tension and compression springs at the wall joints on the ends and shear springs in the center were placed as nonlinear elements.

As regards the tension springs at tensile bolts, the springs of the following three elements in series were used as the initial stiffness (K_{CTB}) for calculation in accordance with the Japanese CLT Manual: the initial stiffness caused by the bearing stress of the timber immediately under the washers for the tensile bolts (K_C), the initial stiffness caused by the tension of the timber at the both ends of notches (K_T) and the tensile axial stiffness of the tensile bolts (K_B), where they are arranged so that the strength might depend upon the tensile yield of tensile bolts without causing the prior tensile or shear failure of CLT to occur around the square holes. The elastic-plastic properties were modelled to be bilinear.

The compression springs in the bearing area were modelled to be bilinear, by calculating the bearing spring stiffness (K_P) on the assumption that the bearing stiffness per unit area (k_c) was 15.6 N/mm^3 for the bearing area of $0.25d \times t$ and then calculating the compression stress (P_{PY}) from the compressive strength (F_c), in compliance with the Japanese CLT Manual [1].

The shear springs at the shear joints, using the yield strength per piece of drift pin shown in Section 2.3, were considered to be rigid (K_{SI}) until the frictional force (P_F) based on the assumption that the friction coefficient was 0.3 against the compressive strength of the bearing area. After that, the stiffness according to the number of drift pins (K_{S2}) was given, and they became trilinear type with a break point at the strength (P_{SY}) as a result of adding the yield strength of drift pins (P_{DPY}) to P_F . Although the tensile and compression spring elements were placed at the nodes of corners of wall panels for the sake of simplicity, the spring stiffness and strength require corrections (reduction) in consideration for the effect of the actual stress positions. By referring to the Japanese CLT manual [1], we set the correction factor (R) to $0.83d/D$, and multiplied the stiffness by R^2 and the strength by R .

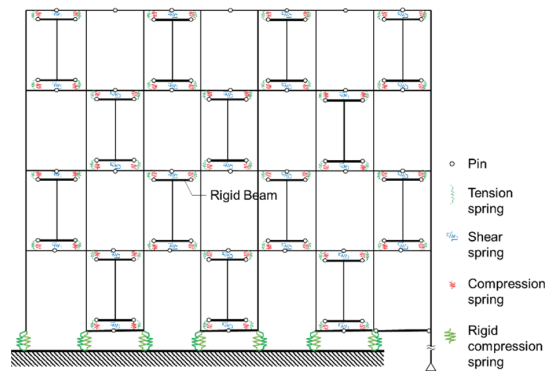


Figure 8: Overview of stress analysis model

Table 2 shows the calculation results for the joint springs in the standard configuration in Figure 4 by using the above procedure. A steel frame was modelled with linear elements, and the bilinear elastic-plastic properties were defined at the member ends. Although the shear yield of steel beams occurs due to the features of CLT panel layout in this structural system, the authors referred to the Reference [5] for the restoring force characteristics against the shear yield of steel plate reinforced by stiffeners and set the decreasing rate of the shear stiffness from the initial stiffness after the shear yield to 0.015.

Table 2: Joint element springs

Compression spring		Tension spring		Shear spring	
k_c (N/mm ²)	15.6	K_c (kN/mm)	101.9	μ	0.3
d (mm)	1855	K_{CT} (kN/mm)	1767.8	$P_F(=\mu \cdot P_{PY})(kN)$	202.8
0.25d (mm)	464	K_{CT} (kN/mm)	96.3	DP	$\phi 16$
t (mm)	150	Tensile bolt diam.	M20	n_s (pcs.)	11
F_c (N/mm ²)	9.72	A_s (mm ²)	260	q_{dpy} (kN/pc.)	22.7
K_p (kN/mm)	1085.2	n_b (pcs.)	2	k_s (kN/mm/pc.)	13.00
P_{PY} (kN)	676.1	L_b (mm)	478	P_{dpy} (kN)	249.7
		K_a (kN/mm)	223.0	K_{S1} (kN/mm)	10000.0
		K_{CTB} (kN/mm)	67.3	K_{S2} (kN/mm)	143.0
		P_{BY} (kN)	115.1	P_{SY} (kN)	452.5

Table 3: Stress analysis results

Direction	Story deformation angle (rad)	Modulus of eccentricity	Story stiffness ratio	Shear force sharing rate of CLT (%)	Mean shear stress of CLT (N/mm ²)
X-direction	1/494 (FL level 4)	0.13 (FL level 4)	0.74 (FL level 4)	79.1 (FL level 2)	0.36 (FL level 2)
Y-direction	1/469 (FL level 2)	0.12 (FL level 3)	0.74 (FL level 2)	84.9 (FL level 2)	0.40 (FL level 2)

2.6 STRESS ANALYSIS RESULTS

Table 3 shows the stress analysis results. In the primary design, the shear force sharing rate of a CLT infill seismic wall is as high as about 80%, the story deformation angle could be also reduced to slightly less than 1/500, smaller than the target value 1/200. Thus, the results indicated that the stiffness of a CLT infill seismic wall was fully contributory.

2.7 HORIZONTAL LOAD-CARRYING CAPACITY CALCULATION

For the Hyogo Forestry Hall, the authors developed the above stress analysis model, and then performed static elasto-plastic analysis and calculated the horizontal load-carrying capacity as shown by the flow diagram in Figure 7, where the problem was how to set the required horizontal load-carrying capacity. There were no experimental findings about the deformation performance and energy absorption of a hybrid structure with CLT seismic panels and a steel frame. Therefore, we reduced the building to an equivalent single-degree-of-freedom (SDOF) system (Figure 9) and then calculated the reduction rate of the required horizontal load-carrying

capacity (structural characteristics factor: D_s) from the equation on the assumption of the property of energy conservation with ductility factor. The seismic force based on the Building Standards Act of Japan was caused to act on each floor (P_i), which was followed by static elasto-plastic analysis, where the horizontal displacement distribution on each floor in each step was reduced to the representative displacement Δ and acceleration A of an equivalent single-degree-of-freedom system (Equations (1) and (2)). If you set a freely-selected target displacement Δn against this $A-\Delta$ curve and establish an energy-equivalent, perfect elasto-plastic model, then that determines the ductility factor (μ), and the value of structural characteristics factor (D_s) to calculate the required horizontal load-carrying capacity (Q_{un}) will be calculated in Equation (3) based on the property of energy conservation (Equations (3) and (4)). From this relationship between a freely-selected target displacement Δn and the D_s value, the acceleration (A_n) equivalent to the required horizontal load-carrying capacity converted into acceleration can be obtained. The intersection between this $A_n - \Delta n$ curve and the $A-\Delta$ curve becomes a point to determine the horizontal load-carrying capacity.

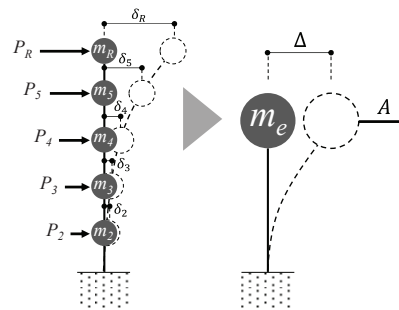


Figure 9: SDOF System

$$A = Q_B \cdot \frac{\sum m_i \cdot d_i^2}{(\sum m_i \cdot d_i)^2} \quad \dots(1)$$

$$\Delta = \frac{\sum m_i \cdot d_i^2}{\sum m_i \cdot d_i} \quad \dots(2)$$

$$D_s = \frac{1}{\sqrt{2\mu - 1}} \quad \dots(3)$$

$$\mu = \frac{\Delta_u}{\Delta_y} \quad \dots(4)$$

$$Q_{un} = D_s \cdot F_{es} \cdot Q_{ud} \quad \dots(5)$$

where Q_B = story shear force of the lowest floor, m_i = mass of the level- i floor, d_i = displacement of the level- i floor, Δ_y, Δ_u = yield displacement and ultimate displacement of perfect elasto-plastic model, bilinear (refer to Figure 12), Q_{un} = required horizontal load-carrying capacity, F_{es} = shape factor (1 in this case) and Q_{ud} = story shear force when the base shear coefficient is 1.

Figures 10 and 11 respectively show the moment diagram and hinge diagram under the horizontal load-carrying capacity. Figure 12 shows the story shear force - story deformation relationship by floors in the +X direction, and Figure 13 illustrates the acceleration - representative displacement curve of an equivalent SDOF system obtained from Figure 12.

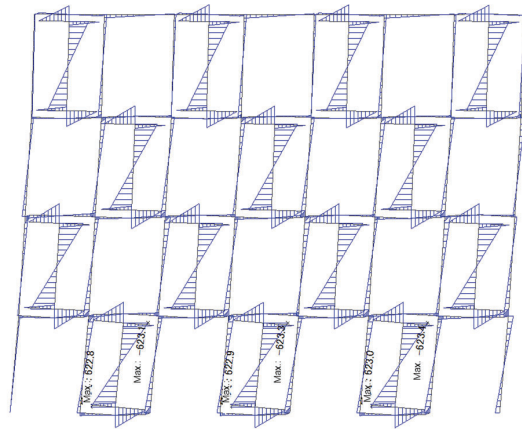


Figure 10: North plane stress diagram (moment diagram) (under horizontal load-carrying capacity, in +X direction)

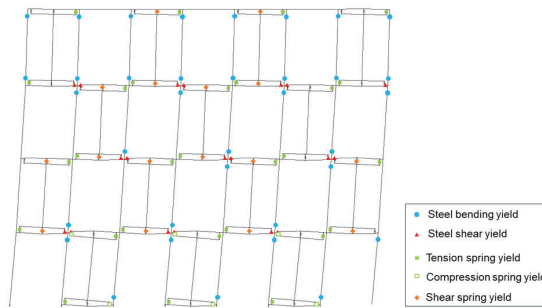


Figure 11: North plane hinge diagram (under horizontal load-carrying capacity, in +X direction)

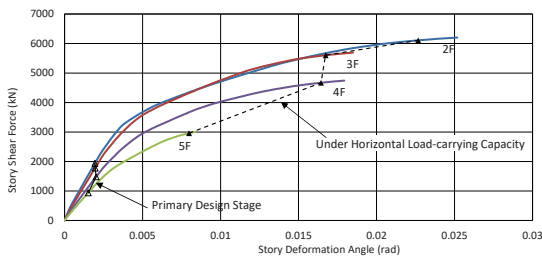


Figure 12: Story shear force - story deformation angle relationship (in +X direction)

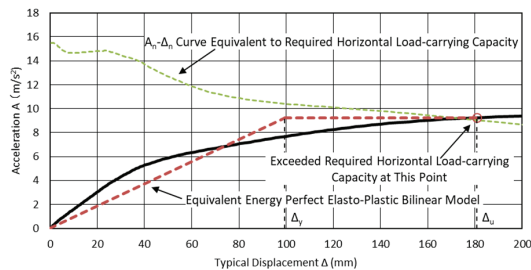


Figure 13: Acceleration - representative displacement relationship (in +X direction)

Table 4: Horizontal load-carrying capacity calculation results

Direction	Story deformation angle (rad)	D_s	F_{es}	Q_{ud} (kN)	Q_{un} (kN)	Q_u (kN) (Qu/Qu)	Shear force sharing rate of CLT (%)	Mean shear stress of CLT (N/mm ²)
+X-direction (FL level 2)	1/44	0.616	1.0	9698	5972	6110	68.9 (FL level 2)	1.05 (FL level 2)
						1.02		
-X-direction (FL level 2)	1/48	0.627	1.0	9698	6077	6110	68.9 (FL level 2)	1.05 (FL level 2)
						1.01		
+Y-direction (FL level 2)	1/46	0.571	1.0	9698	5534	5722	76.6 (FL level 2)	0.99 (FL level 2)
						1.03		
-Y-direction (FL level 2)	1/44	0.606	1.0	9698	5876	5916	77.1 (FL level 2)	1.02 (FL level 2)
						1.01		

The result of performing the horizontal load-carrying capacity calculation for all the cases by the above method was as shown in Table 4, which indicates that the D_s values were between 0.57 and 0.63. The replacement by a bilinear type with an equivalent area has resulted in the calculation result larger than 0.55, the maximum D_s value of RC constructions that is specified in the Building Standards Act of Japan, because of the displacement (Δ_y) increased at yield, preventing the ductility factor (μ) from increasing.

The yields of joints, bending yields of steel columns and shear yields of steel beams occurred as shown by the hinge diagram in Figure 10. Generally, there is a concern of the web buckling in response to the shear force at the steel beam ends. However, as they are reinforced with stiffeners at a spacing of 100 to 140 mm in this case, the shear deformation performance can be expected. As a whole, the behavior with deformation performance is considered to be indicated. Therefore, the D_s values higher than those of strength type RC constructions are slightly unreasonable calculation results, which lacks evidence data to support them in the current situation. Accordingly, performance verification by such means as structure experiments is required in the future.

Furthermore, the sharing rates of the CLT seismic panels under horizontal load-carrying capacity were 68.9 to 77.1%, as shown by the horizontal load-carrying capacity calculation results in Table 4, which shows lower percentages than in the primary design stage. Still, the mean shear stress (τ) was approximately 1.0 N/mm². Finally, it was confirmed that the deformations of the spring models of joint elements at the joints did not exceed the ultimate deformation (δ_u). For the tensile joints, the ultimate displacement was considered to take place at the time when the tensile strain of tensile bolts was 10%. As for the shear joints by the drift pinned joints with insert-steel gusset plates, the ultimate deformation (δ_u) was set to 32 mm in accordance with the experimental results in Reference [4].

3 SECURING FIRE-RESISTANCE PERFORMANCE

Even if used in a fireproof building, CLT seismic panels are not required to have fire-resistance performance under

the Building Standards Act of Japan because they do not support sustained loads but bear only horizontal forces. However, there is a possibility that the CLT seismic panels will continuously self-burn even after the end of fire, and the steel frame to which the panels are installed may be subjected to heating beyond the legally required fire-resistance performance. Hence, the authors performed the full-scale heating test on this structural system to verify the fire-resistance performance. Figures 14 to 16 show the diagram and photos of the full-scale heating test specimens, and Table 5 shows a list of specimens. In the standard configuration shown by Figure 4, the upper part of the vertically divided panel was called the Specimen No. 1, and the lower part was called the Specimen No. 2. The Specimen No. 1 included the assumed CLT floor, which was covered on the upper and lower surfaces with reinforced gypsum boards for fireproofing and installed up to about one meter from the frame center. The space between a CLT seismic panel and a steel beam was filled with 80 mm thick shrinkage-compensating mortar both to transmit compression stress and to cover the beam flanges for fireproofing. We used calcium silicate boards as fireproof covering for the steel of these specimens and gypsum boards for the floor.



Figure 15: Test specimen No. 1



Figure 16: Test specimen No. 2

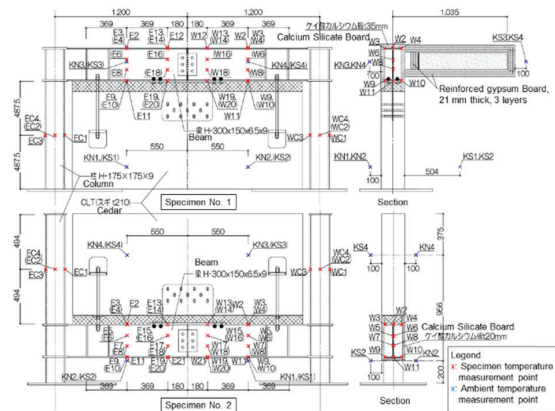


Figure 14: Full-scale heating test specimen diagram

Table 5: List of full-scale heating test specimens

Specimen No.	Steel column	Steel beam	Fireproof covering (Calcium silicate board)
No. 1	□-175x175x9 (STKR400)	H-300x150x6.5x9 (SS400)	Column: 1 hr. (20 mm) Beam: 2 hrs. (35 mm)
No. 2	□-175x175x9 (STKR400)	H-300x150x6.5x9 (SS400)	Column: 1 hr. (20 mm) Beam: 1 hr. (20 mm)

Figures 17 to 20 show the temperature histories at the measuring points of the specimens (the measuring points with the W-codes shown in Figure 14 represent the beam measurement results). It was confirmed that the CLT seismic panels of the both specimens reburned two to four hours after the end of heating and that the ambient temperatures of the specimens rose again up to about 700 degrees Celsius, and the CLT seismic panels burned down about one hour after that. This re-increase of the ambient temperatures after the end of heating is considered to have

been attributable to the fact that the continuous burning from the both sides of the CLT seismic panels even after the end of heating turned into violent reburning when penetrating the CLT seismic panels. For the Specimen No. 1, we reinforced the fireproof covering of the beams to achieve 2-hour fire rating against the temperature rise of the CLT seismic panels due to reburning, which resulted in reducing the beam steel temperature to about 230 degrees Celsius. Consequently, the temperature dropped after reaching the peak 360-420 minutes after the start of heating. Though a temporary rise in the temperature was observed immediately after 60 minutes have passed since the start of heating, that was caused by the hot air that entered through the corners of the floor's butt ends which normally were not heated surfaces. The tensile bolts and shear joints that join CLT seismic panels to steel beams become thermal bridges and cause the steel temperatures to rise. However, keeping 80 mm thick shrinkage-compensating mortar limits the temperatures near the joints (W19 and W20 of No. 1 and W13 and W14 of No. 2) to about 250 degrees Celsius and consequently reduces the effect of the thermal bridges to be minor.

As described above, the maximum temperature of steel after heating for 60 minutes becomes about 450 degrees Celsius, which is considered to have the remaining strength beyond this building's stress due to sustained loading.

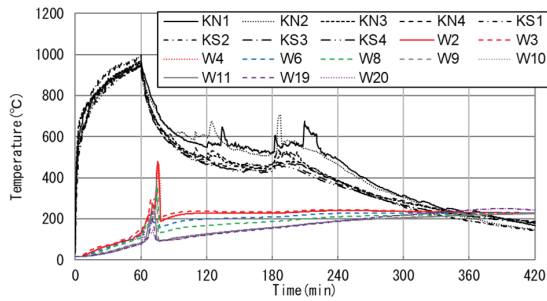


Figure 17: Heating test results (Beam, Specimen No. 1)

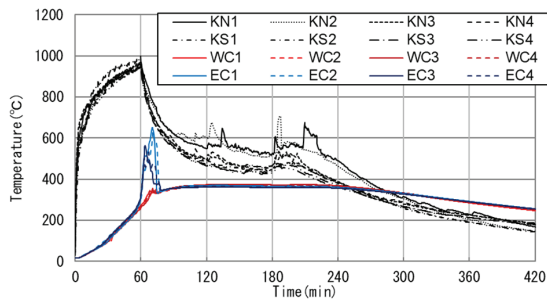


Figure 18: Heating test results (Columns, Specimen No. 1)

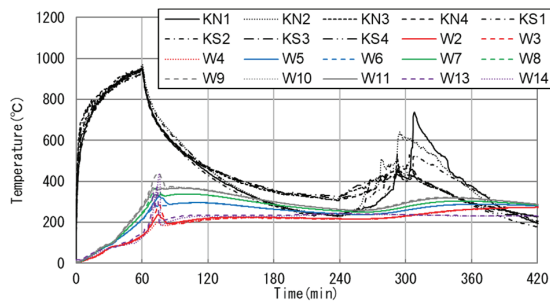


Figure 19: Heating test results (Beam, Specimen No. 2)

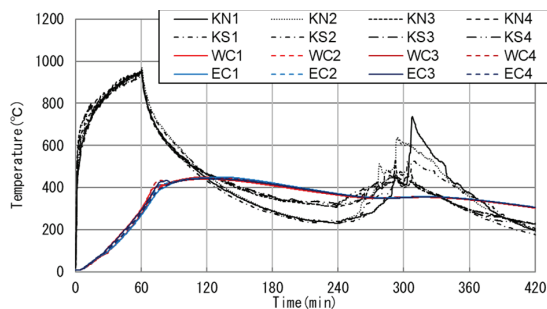


Figure 20: Heating test results (Columns, Specimen No. 2)
 *For the codes showing the measurement points in the specimens in Figures 16 to 19, refer to Figure 13.

4 CONSTRUCTION OF JOINTS

4.1 JOINTS TO TRANSMIT TENSION STRESS (TENSILE BOLT JOINTS)

Figure 21 shows the joint detail of a CLT and steel hybrid structure. Tensile bolts are placed at the four corners of the CLT infill seismic wall to transmit the tension stress

generated due to the bending stress of the wall, and joined to the steel beam flanges.

As shown in Figure 22, the upper and lower surfaces of a CLT panel are filled with shrinkage-compensating mortar to transmit the compression stress and to provide steel beams with fire-resistance performance against the burning of CLT in case of fire as described in Chapter 3. A preliminary execution test was performed on the filling properties of shrinkage-compensating mortar, which verified that the mortar enabled the filling close to 100%.



Figure 21: Tensile bolt joint



Figure 22: Shrinkage-compensating mortar



Figure 23: Shear joint

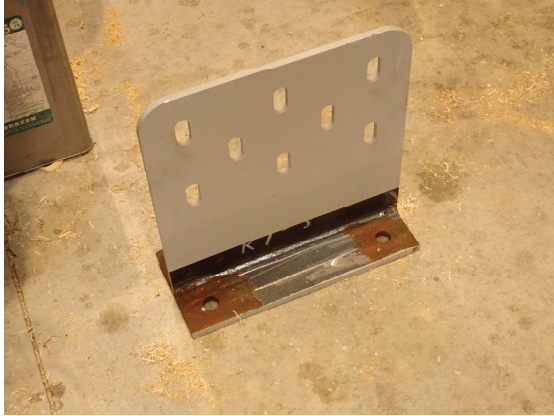


Figure 24: Shear joint

4.2 JOINTS TO TRANSMIT SHEAR STRESS (SHEAR JOINTS)

Refer to Figures 23 and 24. The drift pinned joints with insert-steel gusset plates are used to transmit the shear stress. The insert-steel gusset plates are joined to the steel beam flanges through baseplates with high strength bolts. The drift pin holes in the insert-steel gusset plates are vertically loose so as not to be affected by the rotational deformation caused by the bending of a CLT panel and to allow level adjustments during construction.

4.3 JOINTS OF CLT FLOOR PANELS

Figures 25 and 26 show the joints of the CLT floor panels to the steel beams. The CLT floor panels are placed on the angle brackets installed on the steel beam webs and fixed with wood screws from the underside of the angles. Installation of angle brackets enables alignment of the CLT floor panels with the top level of the steel beams, which contributes to an increase in the effectiveness to the floor height. Besides, since wood screws do not require prepared holes, there is no need for strict precision management during construction. Hence, use of wood screws brings a great improvement in the construction efficiency during erection, compared with the cases of using drift pins or bolts.

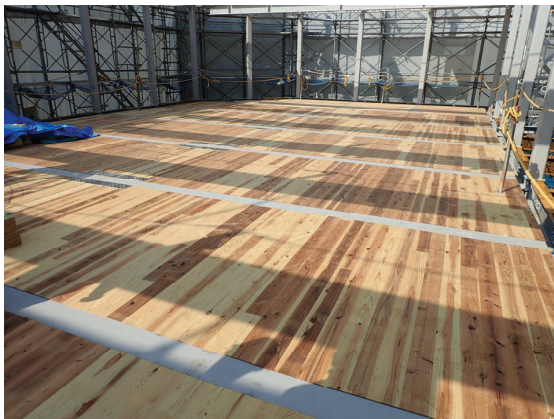


Figure 25: CLT floor panels



Figure 26: CLT-floor-panel to steel-beam joint

Thus, the joints between the CLT panels and steel frame of this building have contributed to the establishment of joining methods in consideration of fire-resistance performance and workability as well as the enhancement of the structural performance.

5 CONCLUSIONS

The above discussion shows that incorporation of CLT seismic panels into a steel frame makes it possible to exhibit the structural performance of the CLT panels efficiently. Additionally, this paper presents a series of structural design method including horizontal load-carrying capacity calculation through an actual case of design and confirms the usefulness of this structural system including fire-resistance performance.

REFERENCES

- [1] Japan Housing and Wood Technology Center: Design and construction manual of building using CLT, 2016. 10 (in Japanese)
- [2] Naturally wood and Forestry Innovation Investment. :Brock Commons Storyboards Factsheet.(online), available from <https://www.naturallywood.com/wp-content/uploads/2020/08/brock-commons-storyboards_factsheet_naturallywood.pdf> (accessed 2021.4.19)
- [3] Bezabeh, M. Tesfamariam, S. and Stierner, S.: Equivalent viscous damping for steel moment-resisting frames with cross-laminated timber infill walls, *Journal of Structural Engineering, ASCE*, DOI: 10.1061/(ASCE)ST.1943-541X.0001316. 2015
- [4] Nakashima, S., Masuda, H., Fujishiro, A., Nonaka, H., Morimoto, T., Otsuka, K.: Development of CLT Drift Pinned Connection for Low-rise Timber Structure, *Summaries of Technical Papers of Annual Meeting, Architectural Institute of Japan, Structures III*, pp. 417-418, 2018.7 (in Japanese)
- [5] Takahashi, Y. and Shinabe, Y.: Experimental Study on Restoring Force Characteristics of Shear Yielding Thin Steel Plate Elements, Buildings, *Journal of Structural and Construction Engineering (Transactions of AIJ)*, Vol. 62, No. 494, pp. 107-114, 1997.4 (in Japanese)